

# Integrating Odometry and Inter-vehicular Communication for Adaptive Cruise Control with Target Detection Loss

Yuan Lin<sup>1</sup>, Chaoxian Wu<sup>2</sup>, and Azim Eskandarian<sup>3</sup>

**Abstract**—Adaptive Cruise Control (ACC) systems utilize distance sensors and control algorithms to enable a vehicle to follow its preceding vehicle with desired headways. There are situations when distance sensors may lose the target, i.e., the preceding vehicle, when unfavorable weather conditions result in low reflectance or the preceding vehicle escapes the sensor's angle of view on curvy roads. In these situations, a common strategy is to suppress acceleration and maintain current speed (Cruise Control) until the sensor detects the preceding vehicle again. In this paper, we propose a new solution which integrates odometry and inter-vehicular communication to enable vehicle following for the period of target detection loss. With inter-vehicular communication, a following vehicle can obtain the odometry data of its preceding vehicle to compute the inter-vehicle distance. This work focuses on the design of an ACC system that can enable vehicle following during short-term target detection loss. The feasibility of the system design is validated through mobile robot experiments. Autonomous lane keeping capability is developed such that the mobile robots move according to the center of the lane. The robot following experiment results show that with accurate odometry and lane centering, the proposed system design can maintain desired headway following.

## I. INTRODUCTION

ACC systems are commercially available in modern vehicles to enable vehicle following with desired headways [1]. ACC systems utilize distance sensors such as radar and lidar to obtain the actual inter-vehicle distance between the vehicle itself and the preceding vehicle [2]. The ACC longitudinal control algorithms minimize the error between the actual and desired inter-vehicle distances for desired following performance [3], [4], [5]. The desired distance can be constant or velocity-dependent [6]. The velocity-dependent desired distance depends on the speed of the following vehicle and thus increases as vehicle speed increases. This abides with safety concerns that high speed driving requires larger inter-vehicle distance. ACC systems allow vehicle to automatically brake and accelerate for desired headway keeping, which leads to leveled-up autonomy as compared to cruise control in that vehicle speed is fixed [7]. Vehicle following with closer headways also contributes to fuel economy, especially for trucks, as aerodynamics drag

becomes smaller [8]. What's more, a large number of ACC vehicles forming dense platoons on the highway can improve traffic throughput [9].

ACC systems may suffer from target detection loss due to sensor and environment issues. A radar sensor has limited angle of view and would miss the target, i.e., the preceding vehicle, on curvy roads, especially in urban driving environment for full speed range ACC [10], [11], [12]. With unfavorable weather conditions such as fog, the reflectance would be low and the sensor may also lose the target [13], [14]. For these situations with short-term target detection loss, it's suggested that the acceleration be suppressed until the sensor detects the target again [10], [11], [12], [15]. It's possible, however, that the preceding vehicle enters ramp and exits highway which can also lead to loss of target detection. Thus, on a curvy road with target detection loss, it has been proposed that the following vehicle travels through the curve for target re-detection purpose to determine whether to continue ACC (target detected again) or not [11], [15].

Next-generation vehicles will be equipped with wireless communication such that they can be connected with each other, infrastructure, and smart phone devices [16], [17]. Vehicle-to-vehicle (V2V) wireless communication, in particular, offers huge benefits to improve traffic safety (such as blind spot warning [18]) and mobility (such as eco-routing [19]). With V2V communication, vehicles can share vehicle states such as acceleration, velocity, and position [20]. In the US, connected vehicles will be using Dedicated Short Range Communication (DSRC) which is a short-to-medium range wireless communication capability allocated in the 5.9 GHz frequency band.

Recent advances in inertial navigation systems can provide accurate localization, position, and odometry data for vehicles [21]. It has been demonstrated that sensor fusing algorithms that fuse GPS, IMU, odometry, and lidar data can provide positioning data with centimeter-scale accuracy [22]. Commercially available inertial navigation systems such as Applanix POS LV can provide positioning data with error less than 1 meter even in the presence of 1-minute GPS outage.

This work here proposes a solution that can enable ACC vehicle following during short-term target detection loss. In our proposed solution, a following vehicle can compute the inter-vehicle distance using the front vehicle's odometry obtained through wireless communication. We validated the solution using autonomous mobile robots programmed with ACC, lane keeping, and wireless communication capabilities. This work explores the use of vehicle connectivity to ac-

<sup>1</sup>Yuan Lin is a postdoctoral research associate in Mechanical Engineering at Virginia Tech, Blacksburg, VA 24061. yuanlin@vt.edu

<sup>2</sup>Chaoxian Wu is a doctoral student at the Hubei Key Laboratory of Advanced Technology for Automotive Components, Automobile Engineering Institute, Wuhan University of Technology, Wuhan, Hubei Province, China 430000. He is also a visiting scholar in Mechanical Engineering at Virginia Tech, Blacksburg, VA 24061. cxw@vt.edu

<sup>3</sup>Azim Eskandarian is a professor and the Department Head of Mechanical Engineering at Virginia Tech, Blacksburg, VA 24061. eskandarian@vt.edu

commodate sensor detection failure so as to provide another safety towards building more reliable ACC.

## II. PROBLEM FORMULATION

Traditional ACC systems rely on distance sensors to detect the preceding vehicle to obtain the inter-vehicle distance. The problem formulation for these systems have been well studied. This section focuses on explaining the problem formulation of ACC system using odometry and wireless communication for the case of target detection loss, see Fig. 1.

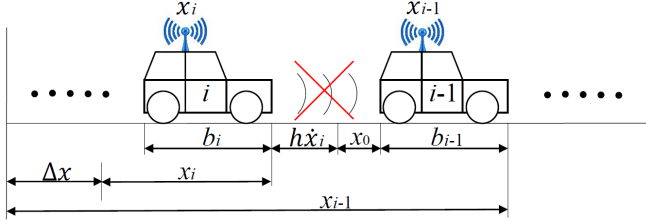


Fig. 1. A schematic for ACC vehicle following using odometry and inter-vehicular wireless communication.  $x_{i-1}$  and  $x_i$  are the odometry readings of the preceding  $i-1$  and following  $i$  vehicles, respectively.  $\dot{x}_i$  is the velocity of the following vehicle  $i$ .  $\Delta x$  is the difference between the odometry reading starting points of the two vehicles.

The odometry readings of the preceding  $i-1$  and following  $i$  vehicles are denoted as  $x_{i-1}$  and  $x_i$ , respectively. We assume that these odometry data are obtained using commercially available state-of-the-art inertial navigation systems and thus reflect accurate distances traversed by the vehicles. It's important to know that every vehicle has unique odometry reading due to the distance it travels from its production up to date. Mathematically, it means that the odometry for different vehicles have different starting points on the same axis, see Fig. 1. A constant  $\Delta x$  is used to denote the difference between the odometry reading starting points of the two vehicles. Then the actual inter-vehicle distance can be calculated as

$$d_i = x_{i-1} - x_i - \Delta x - b_{i-1} \quad (1)$$

where  $b_{i-1}$  is the body length of the preceding vehicle.

In the moment when target detection loss occurs, the odometry readings are denoted as  $x_{i-1}^*$  and  $x_i^*$  and the last sensor measurement of the actual distance is denoted as  $d_i^*$ . Then we have

$$d_i^* = x_{i-1}^* - x_i^* - \Delta x - b_{i-1} \quad (2)$$

As the two vehicles continue to move during the target detection loss period, the actual inter-vehicle distance  $d_i$  can be computed as

$$d_i = x_{i-1} - x_i - (x_{i-1}^* - x_i^* - d_i^*) \quad (3)$$

The following vehicle  $i$  obtains the preceding vehicle's odometry reading  $x_{i-1}$  through wireless communication. In order for  $d_i$  to be accurate, we not only demands that accurate odometry data are obtained using inertial navigation system, but also that both vehicles share the same moving trajectory

which is the center of the lane. This is because even for the same road, if vehicles move with different trajectories (not exactly on the center of the lane), the distances they traverse are different. Thus, autonomous lane centering is the necessary assumption for the entire system design here. However, as we are coping only short-term target detection loss, slightly different moving trajectories may not lead to large errors.

The desired distance  $d_i^d$  is based on a time headway setting. It has two portions: a constant standstill safety distance  $x_0$ , and a velocity-dependent distance  $h\dot{x}_i$  where  $h$  is the time headway and  $\dot{x}_i$  is the velocity of the following vehicle. That means,  $d_i^d = x_0 + h\dot{x}_i$ . The control goal for ACC is to minimize the error between the actual and desired distances  $e_i = d_i - d_i^d$ .

## III. CONTROL SYSTEM BLOCK DIAGRAM

The control system block diagram for the ACC system that integrates odometry and inter-vehicular communication is similar to a traditional ACC system that uses distance sensor, see Fig. 2. The only difference is that the inter-vehicle distance is obtained using odometry with the help of wireless communication. The ACC controller is a feedback controller which takes in the error between the actual and desired distances and generates the acceleration control input  $u_i$  to the vehicle plant.

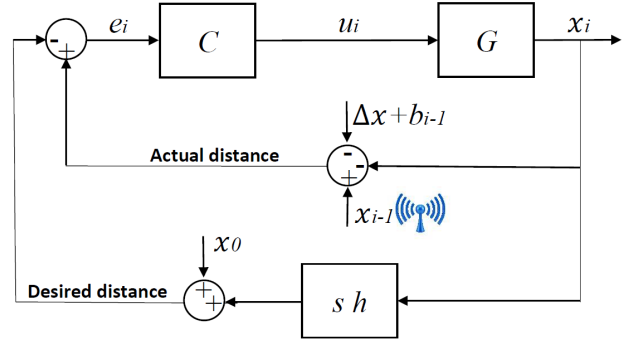


Fig. 2. Block diagram of the ACC system that integrates odometry and inter-vehicular communication.  $C$  is a feedback controller.  $G$  is the vehicle dynamics model.  $h$  is the desired time headway for following.

## IV. SYSTEM DESIGN

A complete ACC system should be able to switch between using distance sensor and odometry to compute inter-vehicle distance. While the default is to use distance sensor for most occasions, the system switches to using odometry when there is short-term target detection loss. The system design is shown using a flow chart in Fig. 3.

## V. ROBOT EXPERIMENT PREPARATION

The feasibility of the system design is validated through mobile robot experiments. The first effort is to develop a working traditional ACC system that relies on distance sensors. Then we emulate the scenario of target detection loss when the system uses odometry to compute inter-vehicle

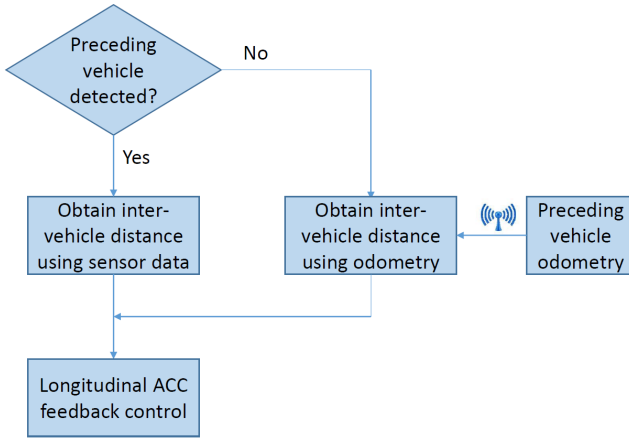


Fig. 3. Flow chart for the complete system design that can switch between using distance sensor and odometry to compute inter-vehicle distance for ACC vehicle following.

distance. All the system development and testing are done via our robotic platform as we use mobile robots to emulate self-driving cars.

#### A. Hardware Preparation

The mobile robots are differential-drive skid-steering robots, Wifibot Lab V4 developed by Nexter Robotics, see Fig. 4. The robots have a low-level micro-controller that reads Infrared (IR) distance sensor measurement and controls the motor speed. White paper boards are used for better IR sensor reflectance such that the IR sensor can obtain stable distance measurements. The micro-controller also reads motor encoder so as to obtain the motor speed and odometry data. For our robot experiments, the odometry data is not corrected with an inertial navigation system since we conduct only in-lab experiments and outdoor GPS information is not available. As the mobile robots suffer minimal wheel slippage on the ground inside the lab, the direct encoder odometry data is sufficient for our robot experiment demonstration.

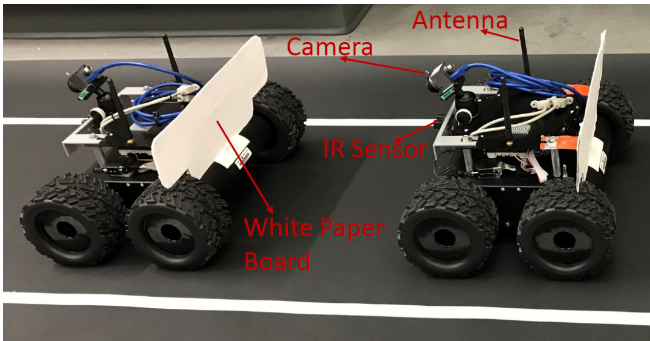


Fig. 4. Two robots that are used for the ACC system testing.

The robots also have a high-level mini-computer with Intel Core I5 CPU. Ubuntu Linux system is installed on the mini-computer. C++ language with Qt as the IDE is used to program the entire high-level ACC control system.

The robot motors take in velocity commands from the micro-controller. Thus, the ACC controller output, the target acceleration, is integrated to obtain velocity to be sent from the mini-computer to the micro-controller via RS232 serial communication for motion control.

#### B. Lane Keeping

As real cars move within lanes, we develop basic lane keeping capability for the robots. The lane keeping capability includes lane detection using computer vision and path following control. For lane detection, we use a fisheye camera to obtain images and C++ and OpenCV libraries for real-time image processing. The outcome of the image processing provides the center of the lane on the image for path following control. The image processing includes the steps of camera calibration to undistort the fisheye images, edge detection to obtain a gray-scale image with lanes appearing as bright pixels, and inverse perspective mapping to obtain a top view of the lane. Using the inverse perspective (top view) images, we relate the images with ground truth, i.e., finding the equivalent real-world length for one pixel, by comparing the length of the same object on the image and in the real world. The lanes are detected as bright pixels on the image and the center locations of the lane are thus computed. To remove error detections, the lane width is checked and extreme slopes of lanes are rejected.

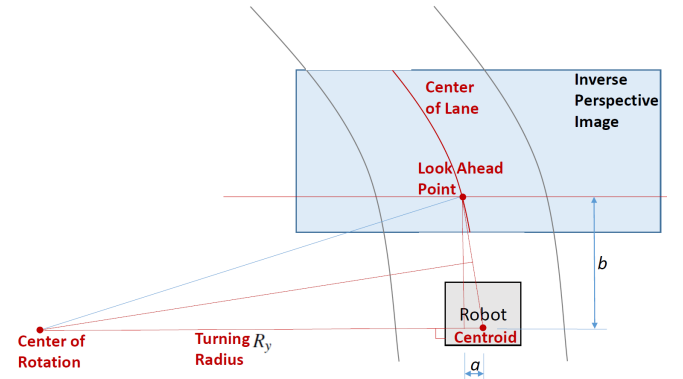


Fig. 5. Schematic for pure pursuit control of the mobile robot.

Pure pursuit control is the path following algorithm to enable the robot to track the center of the lane. For pure pursuit control, there are two major steps: (1) determine the turning radius by defining a look-ahead distance; (2) adjust the left and right wheel velocities to achieve the turning radius based on robot kinematics. Fig. 5 shows the schematic to determine the turning radius using geometry. With a certain look-ahead distance  $b$  measured from the robot centroid, we define a look-ahead line that is parallel to the image or robot width direction. Note that the camera is mounted in the middle of robot width facing the robot length direction. The look-ahead line and the center of the lane intersects at the look-ahead point. We assume that the desired center of rotation is on the line that connects the robot centroid and that is parallel to the robot width direction. As

we use the center of rotation, look-ahead point, and robot centroid to form a circle with the center of rotation as the circle center, the turning radius is obtained using similar triangles as

$$R_y = \frac{a^2 + b^2}{2a} \quad (4)$$

where  $a$  is the lateral distance between the robot centroid and the look-ahead point. When  $a = 0$ , the turning radius  $R_y = \infty$ . In this case, no turning is required. Thus, the left  $v_{1x}$  and right  $v_{2x}$  wheel velocities are equal to the longitudinal average velocity at the centroid  $v_x$ .

Note that the literature has shown that the actual center of rotation of the robot is a little off the line that connects that centroid and that is parallel to the width direction when robot dynamics is considered. However, the offset is small and the center of rotation always remains within the two parallel lines that extend from the robot front and end. Thus, we neglect this offset as the focus of the work is not on the accuracy of the path following.

With the computed turning radius  $R_y$ , we obtain the left  $v_{1x}$  and right  $v_{2x}$  wheel velocities using just robot kinematics, see Fig. 6. The left two wheels have the same velocity as  $v_{1x}$ , so are the right two wheels as  $v_{2x}$ . The longitudinal average velocity at the centroid  $v_x = (v_{1x} + v_{2x})/2$  is determined by the ACC feedback control system. Note that the ACC feedback controller generates target acceleration which is further integrated to obtain  $v_x$ . The robot kinematics equations include  $v_{1x} = (R_y - c)w$ ,  $v_{2x} = (R_y + c)w$ , and  $v_x = R_y w$ . The variable  $c$  is half of the robot width between the middle lines of left and right robot wheels, see Fig. 6. Thus, the left and right wheel velocities for certain turning radius  $R_y$  and longitudinal average velocity  $v_x$  are

$$\begin{aligned} v_{1x} &= \left(1 - \frac{c}{R_y}\right)v_x \\ v_{2x} &= \left(1 + \frac{c}{R_y}\right)v_x \end{aligned} \quad (5)$$

where  $w$  is the angular velocity.

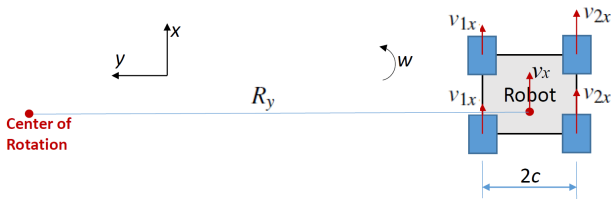


Fig. 6. Schematic for robot kinematics.  $w$  is the angular velocity.  $R_y$  is the robot turning radius.  $v_{1x}$  is the velocity of the left two wheels;  $v_{2x}$  is the velocity of the right two wheels.  $v_x$  is the velocity at the robot centroid.

### C. Inter-vehicular Communication

The decentralized wireless communication, ad hoc, which enables direct node to node communication is implemented for inter-vehicular communication. The robots are equipped with 802.11a/b/g Qualcomm Atheros AR93xx WLAN interface card and antenna. The wireless communication is enabled using User Datagram Protocol (UDP) socket through

C++ programming. The communication is operated at 2.4 GHz band with sending or receiving rate at 100Hz. In-lab experiments have shown that there is no communication package loss.

Each robot has a unique IP address and stores its predecessor and follower's IP addresses in the controlled experiments. The preceding robot sends data exclusively to the following robot and the following robot receives data exclusively from the preceding robot. Note that, in real-world driving, it may be challenging for a car to obtain its predecessor and follower's wireless IDs from many connected cars traveling by. However, in real-life inter-vehicular communications, it is possible to have a relative positioning algorithm with temporary designation ID tags to identify the surrounding vehicles as long as they are engaged in the current car following or platooning activities. This needs to be implemented additionally in the future to our current algorithm.

### D. Parameter Determination

The direct sensor measurements which include the IR sensor distance measurement and motor encoder speed measurement contain high-frequency noise and are filtered using first-order low-pass filters. We convert initial time-domain measurements to frequency-domain representation through Fourier Transform and then select appropriate cut-off frequencies to reduce the high-frequency components of the measurement data. For both the distance and speed measurements, the cut-off frequencies are selected as 4 Hz. We choose higher cut-off frequencies as we don't want to introduce large artificial delay to the system. The filtered signal still appears to be a little noisy.

The ACC feedback controller is a Proportional-Derivative (PD) controller. The ACC system with the PD controller does not have steady-state error as we obtain the step response of the system analytically. Due to the scope of this paper, the step response analysis is not provided here. The PD gains are tuned through trial and error based on Ziegler-Nichols' method. Further fine tuning of the PD gains is also adopted to obtain smooth speed and desired rise and settling times. The PD gains are selected as 0.10 and 0.18, respectively.

## VI. ROBOT EXPERIMENT RESULTS

The goal of the robot experiments is to examine the ACC system that uses odometry to compute inter-vehicle distance during target detection loss. We design controlled experiments to compare vehicle following performances for both cases when using distance sensor measurement and when using odometry. Note that when the system uses odometry to compute inter-vehicle distance, the accuracy of the odometry data is the determining factor for successful vehicle following, providing that the robots have lane centering capability. Thus, for one set of the controlled experiments, we deliberately switch from sensor measurement to odometry calculation although the sensor still records the actual distance. In this manner, we can compare the distance calculated using odometry and the recorded actual distance

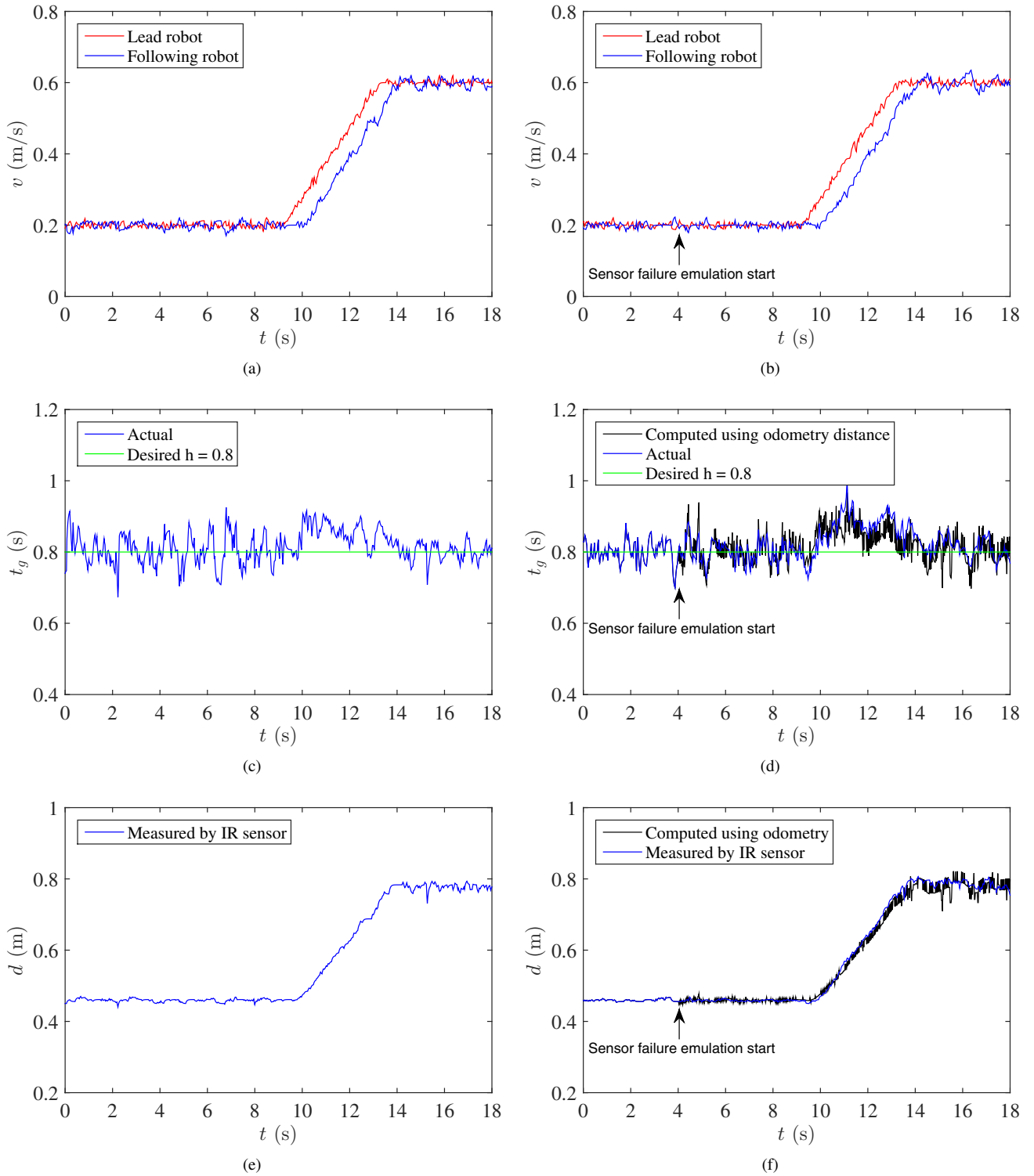


Fig. 7. Robot following results. (a), (c), and (e) are the velocity, time headway, and inter-vehicle distance results for the ACC experiment that uses only IR sensor to obtain inter-vehicle distance. (b), (d), and (f) are the velocity, time headway, and inter-vehicle distance results for the ACC experiment wherein the following robot switches from using IR sensor to using odometry and wireless communication to obtain inter-vehicle distance. Note that after the sensor failure emulation starts, the following robot uses the inter-vehicle distance calculated using odometry to update the ACC control system.

sensor measurement to examine the accuracy of the odometry data.

The robot experiments are conducted on a straight lane as the IR distance sensor has very narrow measurement angle as a one-dimensional sensor. The lead robot's velocity profile is pre-designed and includes constant velocity and acceleration, see Fig. 7. For the first set of the controlled experiments, the following robot uses solely the IR sensor to obtain the inter-vehicle distance. The velocity, time headway, and inter-vehicle distance results are shown on the left three plots of Fig. 7. From these results, we see that the actual time headway is practically the same as the desired time headway  $h = 0.8$  seconds. It means that the PD gains result in satisfying time headway following. Note that the results are noisy due to the noisy sensor measurement data.

For the other set of the controlled experiments, we deliberately switch from using distance sensor to using odometry and wireless communication to obtain the inter-vehicle distance at some point (before acceleration starts) during the experiment. This is to emulate a sensor detection failure scenario while we still record the actual distance using the IR sensor. The right three plots of Fig. 7 show the results of the experiments. From the results, we see that the inter-vehicle distance computed using odometry is roughly the same as that measured by the IR sensor. Consequently, the actual time headway computed using the IR sensor distance is practically the same as or very close to the desired time headway  $h = 0.8$  seconds.

## VII. CONCLUSION

From the robot experiment results, we see that the designed system enables vehicle following for both cases when distance sensor measurement is and is not available. As inter-vehicle distance can be computed using accurate odometry data during target detection loss, the same vehicle following performance could be achieved as when distance sensor measurement is available.

In conclusion, we presented a new solution that can enable vehicle following during target detection loss by using odometry to compute inter-vehicle distance. The solution is based on the assumption that the vehicles have autonomous lane centering capability. In our solution, the following vehicle receives the preceding vehicle's odometry data through inter-vehicular wireless communication. The system design is tested using our autonomous mobile robot platform. The lane centering capability is developed for the robots as cameras are used for lane detection and pure pursuit control algorithm is used for path following control. Future work includes implementing the system design on real cars to test the performance for high speed driving. We would also investigate the impact of wireless communication delay and package loss on the vehicle following performance.

## REFERENCES

- [1] A. Vahidi and A. Eskandarian, "Research advances in intelligent collision avoidance and adaptive cruise control," *IEEE transactions on intelligent transportation systems*, vol. 4, no. 3, pp. 143–153, 2003.
- [2] G. R. Widmann, M. K. Daniels, L. Hamilton, L. Humm, B. Riley, J. K. Schiffmann, D. E. Schnelker, and W. H. Wishon, "Comparison of lidar-based and radar-based adaptive cruise control systems," SAE Technical Paper, Tech. Rep., 2000.
- [3] C.-Y. Liang and H. Peng, "Optimal adaptive cruise control with guaranteed string stability," *Vehicle system dynamics*, vol. 32, no. 4-5, pp. 313–330, 1999.
- [4] B. Ganji, A. Z. Kouzani, S. Y. Khoo, and M. Shams-Zahraei, "Adaptive cruise control of a HEV using sliding mode control," *Expert Systems with Applications*, vol. 41, no. 2, pp. 607–615, 2014.
- [5] J. E. Naranjo, C. González, J. Reviejo, R. García, and T. De Pedro, "Adaptive fuzzy control for inter-vehicle gap keeping," *IEEE Transactions on Intelligent Transportation Systems*, vol. 4, no. 3, pp. 132–142, 2003.
- [6] G. J. Naus, R. P. Vugts, J. Ploeg, M. J. van de Molengraft, and M. Steinbuch, "String-stable CACC design and experimental validation: A frequency-domain approach," *IEEE Transactions on Vehicular Technology*, vol. 59, no. 9, pp. 4268–4279, 2010.
- [7] A. Eskandarian, *Handbook of intelligent vehicles*. Springer London, 2012.
- [8] A. Al Alam, A. Gattami, and K. H. Johansson, "An experimental study on the fuel reduction potential of heavy duty vehicle platooning," in *2010 13th International IEEE Conference on Intelligent Transportation Systems (ITSC)*. IEEE, 2010, pp. 306–311.
- [9] B. Van Arem, C. J. Van Driel, and R. Visser, "The impact of cooperative adaptive cruise control on traffic-flow characteristics," *IEEE Transactions on Intelligent Transportation Systems*, vol. 7, no. 4, pp. 429–436, 2006.
- [10] F. Ahmed-Zaid, G. H. Engelman, and P. R. Haney, "Object detection in adaptive cruise control," Nov. 22 2005, US Patent 6,968,266.
- [11] H. Sudou and T. Hashizume, "Adaptive cruise control system," Jan. 10 2006, US Patent 6,985,805.
- [12] G. H. Engelman, M. J. Richardson, P. A. Barber, and P. J. King, "Adaptive vehicle cruise control system and methodology," May 15 2001, US Patent 6,233,515.
- [13] P. M. Austin, "Relation between measured radar reflectivity and surface rainfall," *Monthly Weather Review*, vol. 115, no. 5, pp. 1053–1070, 1987.
- [14] J. DiFranco and B. Rubin, *Radar detection*. The Institution of Engineering and Technology, 2004.
- [15] H. Winner, S. Hakuli, F. Lotz, and C. Singer, *Handbook of Driver Assistance Systems: Basic Information, Components and Systems for Active Safety and Comfort*. Springer Publishing Company, Incorporated, 2015.
- [16] J. J. Blum, A. Eskandarian, and L. J. Hoffman, "Challenges of inter-vehicle ad hoc networks," *IEEE transactions on intelligent transportation systems*, vol. 5, no. 4, pp. 347–351, 2004.
- [17] N. Lu, N. Cheng, N. Zhang, X. Shen, and J. W. Mark, "Connected vehicles: Solutions and challenges," *IEEE internet of things journal*, vol. 1, no. 4, pp. 289–299, 2014.
- [18] J. E. Naranjo, F. Jiménez, J. J. Anaya, E. Talavera, and O. Gómez, "Application of vehicle to another entity (v2x) communications for motorcycle crash avoidance," *Journal of Intelligent Transportation Systems*, vol. 21, no. 4, pp. 285–295, 2017.
- [19] A. Elbery, H. Rakha, M. Elnainay, W. Drira, and F. Filali, "Eco-routing using v2i communication: System evaluation," in *2015 IEEE 18th International Conference on Intelligent Transportation Systems (ITSC)*. IEEE, 2015, pp. 71–76.
- [20] Y. Lin and A. Eskandarian, "Experimental evaluation of cooperative adaptive cruise control with autonomous mobile robots," in *2017 IEEE Conference on Control Technology and Applications (CCTA)*. IEEE, 2017, pp. 281–286.
- [21] J. Farrell, *Aided navigation: GPS with high rate sensors*. McGraw-Hill, Inc., 2008.
- [22] J. Levinson and S. Thrun, "Robust vehicle localization in urban environments using probabilistic maps," in *2010 IEEE International Conference on Robotics and Automation (ICRA)*. IEEE, 2010, pp. 4372–4378.